MOLECULAR AND CELLULAR BIOLOGY, Oct. 2007, p. 7089–7101 Vol. 27, No. 20
0270-7306/07/$08.00+0 doi:10.1128/MCB.00838-07

Chromium Cross-Links Histone Deacetylase 1-DNA Methyltransferase 1 Complexes to Chromatin, Inhibiting Histone-Remodeling Marks Critical for Transcriptional Activation[▽]

Michael Schnekenburger, Glenn Talaska, and Alvaro Puga*

Department of Environmental Health and Center for Environmental Genetics, University of Cincinnati Medical Center, P.O. Box 670056, Cincinnati, Ohio 45267-0056

Received 12 May 2007/Returned for modification 25 June 2007/Accepted 26 July 2007

Transcriptional regulation of gene expression requires posttranslational modification of histone proteins, which, in concert with chromatin-remodeling factors, modulate chromatin structure. Exposure to environmental agents may interfere with specific histone modifications and derail normal patterns of gene expression. To test this hypothesis, we coexposed cells to binary mixtures of benzo[*a*]pyrene (B[*a*]P), an environmental procarcinogen that activates *Cyp1a1* transcriptional responses mediated by the aryl hydrocarbon receptor (AHR), and chromium, a carcinogenic heavy metal that represses B[*a*]P-inducible AHR-mediated gene expression. We show that chromium cross-links histone deacetylase 1-DNA methyltransferase 1 (HDAC1-DNMT1) complexes to *Cyp1a1* promoter chromatin and inhibits histone marks induced by AHR-mediated gene transactivation, including phosphorylation of histone H3 Ser-10, trimethylation of H3 Lys-4, and various acetylation marks in histones H3 and H4. These changes inhibit RNA polymerase II recruitment without affecting the kinetics of AHR DNA binding. HDAC1 and DNMT1 inhibitors or depletion of HDAC1 or DNMT1 with siRNAs blocks chromium-induced transcriptional repression by decreasing the interaction of these proteins with the *Cyp1a1* promoter and allowing histone acetylation to proceed. By inhibiting Cyp1a1 expression, chromium stimulates the formation of B[*a*]P DNA adducts. Epigenetic modification of gene expression patterns may be a key element of the developmental and carcinogenic outcomes of exposure to chromium and to other environmental agents.

Contamination of human habitats with complex mixtures of polycyclic aromatic hydrocarbons and heavy metals is a common environmental health problem. Although exposure to background levels of toxic and carcinogenic compounds occurs naturally, exposures at significantly higher concentrations occur in occupational settings with agents coreleased from multiple sources. Primary among these are manufacturing processes and anthropogenic activities, such as fossil fuel combustion, municipal waste incineration, car exhaust, smelter activity, and others. Among the agents involved, chromium and benzo[*a*]pyrene (B[*a*]P) have ranked among the top 20 in the National Priority List of Hazardous Substances (http://www.atsdr.cdc.gov/cercla/05list.html) for as long as this list has been in existence.

B[*a*]P is the model compound of carcinogenic polycyclic aromatic hydrocarbon biotransformation (10). B[*a*]P is activated primarily by the cytochrome P450 CYP1A1 and CYP1B1 enzymes, two heme-containing proteins responsible for the metabolic activation and detoxification of numerous xenobiotics. Bioactivation results in a wide range of oxygenated metabolites, some of which are highly carcinogenic (43). Cytochrome P450-catalyzed reactions lead to both the production and the detoxification of B[*a*]P reactive intermediates, among them 7,8-dihydroxy-9,10-epoxy-7,8,9,10-tetrahydro-B[*a*]P (BPDE), the ultimate carcinogen, which forms adducts with DNA responsible for mutagenesis and carcinogenic initiation. B[*a*]P-mediated induction of CYP1A1 is regulated primarily at the level of transcription through the aryl hydrocarbon receptor (AHR) pathway (53). AHR is a ligand-activated basic region/helix-loop-helix/Per-AHR nuclear translocator (ARNT)-Sim transcription factor sequestered in the cytoplasm in a complex with chaperone HSP90 proteins (21). Upon ligand binding, AHR translocates to the nucleus, dissociates from the chaperones and forms transcriptionally active heterodimers with ARNT (16, 19). AHR-ARNT complexes bind to *cis*-acting AHR response elements (AhRE, XRE, DRE) located in the regulatory regions of target genes of the AHR gene battery, including genes coding for phase I detoxification enzymes such as the cytochromes P450 CYP1A1, -1A2, and -1B1 and phase II enzymes such as NAD(P)H-dependent quinone oxidoreductase 1 (NQO1), glutathione *S*-transferase M1, aldehyde dehydrogenase 3A1 (ALDH3A1), and others (34).

Chromium is also a potent human mutagen and carcinogen (9). Cr(III) is the most prevalent form in the environment and in biological tissues and is generally believed to be an essential element involved in sugar and fat metabolism (5). Cr(VI) is the form more often produced industrially and the one that causes most adverse health effects (8). Cr(VI) is a powerful oxidant that enters cells through the sulfate anion transporter and becomes reduced via Cr(V) and Cr(IV) intermediate oxidation states to the stable Cr(III) form. It is in this process of reduction that Cr(VI) causes its deleterious effects. Exposure to Cr(VI) compounds has been known for over a century to be associated with an elevated

* Corresponding author. Mailing address: Department of Environmental Health, University of Cincinnati Medical Center, P.O. Box 670056, Cincinnati, OH 45267-0056. Phone: (513) 558-0916. Fax: (513) 558-0925. E-mail: Alvaro.Puga@UC.EDU.

▽ Published ahead of print on 6 August 2007.

cancer incidence, particularly squamous cell carcinoma of the lung (14), and other adverse health effects (2, 8).

Intracellular Cr(VI) reduction, which generates reactive oxygen species, has been proposed as the most probable cause of chromium-induced tissue damage, underlying its toxicity and carcinogenicity. Chromium treatment of culture cells results in radical-mediated DNA strand breakage and formation of stable chromium-DNA complexes, including chromium-DNA adducts and protein-chromium-DNA and DNA-chromium-DNA cross-links (56). Chromium exposure often has a repressor effect on the transcription of inducible genes, leaving unaffected the expression of constitutive housekeeping genes (26, 27, 29, 37, 52), perhaps because inducible gene promoters might present a permissive chromatin structure that offers a better target than the promoter of constitutive genes. In addition, chromium-DNA complexes tend to occur preferentially in nuclear matrix DNA (54), where diverse processes take place, including DNA replication, transcription, and RNA processing (4). Cross-linking of the proteins involved in these processes to promoter chromatin is likely to perturb normal chromatin structure regulation and remodeling, causing the disruption of gene expression regulatory patterns (26, 36, 39, 44).

Previous studies from our laboratory have shown that this might be the case. Chromium was found to inhibit activated AHR-inducible *Cyp1a1* and *Nqo1* expression and the expression of over 50 other genes involved in various biological and signaling pathways (50). Inhibition resulted from blocking the release of histone deacetylase 1 (HDAC1) from the *Cyp1a1* promoter and the recruitment of p300 while allowing the AHR complex to bind unimpeded to its cognate motif (50). In the present study, we have explored the hypothesis that chromium disrupts the chromatin remodeling and histone modifications that normally take place after ligand-mediated AHR activation. Chromatin immunoprecipitation (ChIP) assays and quantitative real-time PCR (QRT-PCR) were used to analyze the consequences of chromium treatment for HDAC1-DNA methyltransferase 1 (HDAC1-DNMT1) interactions and histone modifications in the 5′-flanking region of the inducible *Cyp1a1* gene. HDAC1 and DNMT1 inhibitors and depletion of HDAC1 and DNMT1 with small interfering RNA (siRNA) blocked chromium-induced transcriptional repression by decreasing the interaction of these proteins with the promoter and allowing the initiation of histone acetylation associated with *Cyp1a1* gene induction. By inhibiting Cyp1a1 expression, chromium stimulated the formation of BPDE-DNA adducts. We find that chromium causes these effects by cross-linking HDAC1 to chromatin.

MATERIALS AND METHODS

Cell culture and chemical treatments. Mouse hepatoma Hepa-1c1c7 (Hepa-1) cells from the American Type Culture Collection were cultured in α-minimal essential medium (Gibco) supplemented with 5% (vol/vol) fetal bovine serum (Sigma) and 1% (vol/vol) antibiotic-antimycotic (Gibco) in a 5% CO_2 humidified atmosphere at 37°C. Cells were treated when they reached 70 to 80% confluence. A 1,000× concentrated potassium chromate (K_2CrO_4) solution, hereafter referred to as chromium, was dissolved in sterile deionized water and added to the medium at 50 μM final concentration. B[*a*]P at 5 μM was added to the medium in a dimethyl sulfoxide (DMSO) volume not exceeding 0.1% of the total culture medium, which was the volume of DMSO used to treat DMSO vehicle controls. 5-Aza-2′-deoxycytidine (Aza) and sodium butyrate (NaB) were dissolved in DMSO and sterile deionized water, respectively, prior to use. Cells were seeded 24 h before the beginning of treatments and were treated with 2 μM Aza, 2 mM NaB, or both. The medium was supplemented with Aza for a total of 72 h, and at every 12-h interval, spent medium was replaced with fresh Aza-supplemented medium. NaB was added to the medium 16 h prior to termination of the experiments or before treatment with chromium and B[*a*]P. Detailed treatment procedures are given in the following sections or described in the figure legends.

siRNA transfection. siRNAs (Ambion) were transfected by procedures based on the recommended neofection protocol of the manufacturer. siRNA duplexes were used at a final concentration of 25 nM for siGAPDH (glyceraldehyde-3-phosphate dehydrogenase) (catalog no. 4631) and 50 nM for siHDAC1 (catalog no. 61931), siDNMT1 (catalog no. 161527), and the negative control (scrambled; catalog no. 4611). At 48 h posttransfection, either cells were used to measure mRNA and protein expression of siRNA target genes or total RNA was extracted after stimulation with B[*a*]P to measure *Cyp1a1* expression.

Preparation of total protein extracts and Western blotting. At 48 h posttransfection with siRNAs, cells were directly lysed on the plate with 2× loading buffer (0.125 M Tris-HCl [pH 6.5], 20% glycerol, 4% sodium dodecyl sulfate, 5% β-mercaptoethanol, and bromophenol blue). Lysates were boiled for 5 min, run on a 12% polyacrylamide gel, and transferred to Hybond-P membranes (AP-Biotech). Membranes were blocked in 1× phosphate-buffered saline (PBS) containing 0.1% (vol/vol) Tween 20 (PBS-T) and 5% fat-free milk. Primary antibodies were mouse monoclonal anti-HDAC1 (Upstate) or mouse monoclonal anti-β-actin (Sigma), all used in PBS-T containing 5% fat-free milk. Membranes were washed three times for 10 min each in PBS-T before incubation with the appropriate horseradish peroxidase-conjugated anti-rabbit or anti-mouse secondary antibodies (Santa Cruz) in PBS-T containing 5% fat-free milk and were visualized with a chemiluminescent detection reagent (Supersignal West Pico; Pierce).

RNA extraction and cDNA synthesis. Total RNA was extracted using NucleoSpin RNA II columns (Macherey-Nagel) according to the manufacturer's instructions. cDNA was synthesized by reverse transcription of total RNA with SuperScript II RNase H− reverse transcriptase (Invitrogen). An aliquot of the cDNA products was used as the template for subsequent quantification by real-time PCR amplification. Samples were amplified with mouse CYP1A1 primers (forward, 5′-GTGTCTGGTTACTTTGACAAGTGG-3′; reverse, 5′-AACA TGGACATGCAAGGACA-3′), giving a product of 199 bp; HDAC1 primers (forward, 5′-TTCCAACATGACCAACCAGA-3′; reverse, 5′-GGCAGCATCC TCAAGTTCTC-3′), giving a product of 81 bp; GAPDH primers (forward, 5′-AACTTTGGCATTGTGGAAGG-3′; reverse, 5′-GGATGCAGGGATGAT GTTCT-3′), giving a product of 132 bp; and β-actin primers (forward, 5′-CAT CCGTAAAGACCTCTATGCC-3′; reverse, 5′-ACGCAGCTCAGTAACAGT CC-3′), giving a product of 287 bp. Amplification of β-actin cDNA in the same samples was used as an internal control for all PCR amplification reactions.

DNA adduct analysis. Cells were pretreated with the indicated concentrations of sodium chromate for 30 min followed by 1.0 μM B[*a*]P for 2 h or 24 h. Longer treatments were done at lower chromium doses to prevent effects due to cytotoxicity. ^{32}P-postlabeling assays were performed after genomic DNA extractions by standard procedures with modifications described in detail elsewhere (7). Briefly, 2 to 4 μg of DNA was hydrolyzed with 0.25 unit of micrococcal endonuclease and 0.001 unit of calf spleen phosphodiesterase for 3 h at 37°C. The hydrolyzed DNA was digested with 3.5 units of nuclease P1 for 30 min at 37°C, and the adducted nucleotides were subsequently labeled by addition of 50 μCi/sample of [γ-^{32}P]ATP and 2.8 units of polynucleotide kinase and incubation of the reaction mixture for an additional 30 min at 37°C. The postlabeled mixtures were applied to 20- by 20-cm polyethyleneimine-cellulose plates (Alltech). Chromatography was done using a four-solvent system as described previously (45). Adducts were visualized by autoradiography and were quantified by scintillation counting.

Colorimetric histone acetyltransferase activity assays. After the various treatments, cells were harvested and nuclear or total extracts were prepared in a modified radioimmunoprecipitation assay (RIPA) buffer by methods described by others (32). Briefly, after being rinsed twice with ice-cold 1× PBS, cells were scraped from the dishes, pelleted by centrifugation, and resuspended in modified RIPA buffer (50 mM Tris-HCl [pH 7.4], 1% NP-40, 0.25% Na-deoxycholate, 150 mM NaCl, 1 mM EDTA, and 1× protease inhibitor cocktail [Roche]). The cell suspension was gently mixed on an orbital shaker at 4°C for 15 min and centrifuged at 14,000 × *g* at 4°C for 15 min. The supernatant fraction was precleared for 30 min at 4°C with a 50% gel slurry of protein A-agarose beads saturated with salmon sperm DNA and bovine serum albumin (Upstate). Five hundred micrograms of the precleared lysate was incubated for 2 h at 4°C with either anti-HDAC-1 antibody (Upstate) or nonimmune immunoglobulin G (IgG). The immune complexes were recovered by a 2-hour incubation at 4°C with a 50% gel slurry of protein A-agarose beads. Beads were pelleted and washed three times with ice-cold modified RIPA buffer. The protein content was determined for

TABLE 1. PCR primer sequences used in ChIP experiments

Gene	Primer		PCR product size (bp)	Position from +1 (kbp)
	Forward (5′→3′)	Reverse (5′→3′)		
Cyp1a1	TGGGATACCATCAGCTCCAT	AACCTTTGGAAGGTGGAAGG	89	+0.6
	CTCCCTCCCAAGAAAAGGAA	AGCTGATACCTCTGGCCTCA	149	+0.2
	TATCCGGTATGGCTTCTTGC	CACCTTCAGGGTTAGGGTGA	164	−0.1
	AATTTGTGGGGCACAGAGTC	GAACAGCTGGGTGGTGACTT	136	−0.5
	AAGCATCACCCTTTGTAGCC	CAGGCAACACAGAGAAGTCG	122	−0.8
	CTGTTCAGGCCTTTGCTCTC	CTTAAAGGGCCAGCTCTCCT	155	−1.2
	CATCAATCACCAGCATCCAG	TGCTCTGTGACCAAGACCAG	136	−1.5
	ACCCCCTTACCACAACCTCT	CCAGGGGAGTGCTCTCTGA	160	−1.8
	TGGGCAGACCTGGTAGATTC	ACCCCTATTGATCCCCAGAG	176	−2.2
	CCCACCTATAATGCGGTTTG	CATCTTTGCAGCCATTCTCA	151	−2.5
	TCCAGAGATGCAGTGAGTGG	AAAGGGAGGAAGAAGAGGACA	140	−2.9
	CAGAGGTCACTGGGCCTTT	AGGAATGCAGGAAGCCCTAC	131	−3.2
	GCTCTTTCTCTGCCAGGTTG	GGCTAAGGGTCACAATGGAA	227	−3.6
Aldh3a1	GGATGTGATTTTTCTGCCTTTCTTG	GCTGTCTGTTTTGTTCTGTTCTG	261	−0.3
Nqo1	TAAGAGCAGAACGCAGCAC	ACCTGCCTACATAATCAGCC	191	−0.4

each sample using the Bradford assay (Bio-Rad). Measurements of HDAC activity were performed on either 5 μg of nuclear extracts or immunoprecipitated proteins using a HDAC assay kit (Upstate) according to the manufacturer's instructions.

ChIP and PCR analyses. ChIP was performed with minor modifications of the procedure described by Wells and Farnham (51). Approximately 1.5×10^7 to 2×10^7 Hepa-1 cells were incubated for 10 min at room temperature with 1% formaldehyde. After cross-linking, the reaction was quenched with 0.125 M glycine for 10 min at room temperature. After being rinsed twice with ice-cold 1× PBS, cells were scraped from the dishes, pelleted by centrifugation, resuspended in cell lysis buffer (5 mM PIPES [pH 8.0], 85 mM KCl, 0.5% NP-40, and 1× protease inhibitor cocktail [Roche]), and incubated on ice for 10 min. The nuclei were pelleted, resuspended in nucleus lysis buffer (50 mM Tris-HCl [pH 8.1], 10 mM EDTA, 1% sodium dodecyl sulfate, and protease inhibitor cocktail), and incubated on ice for 10 min. Chromatin was sheared to a size range of 0.3 to 0.8 kb by sonication in a crushed-ice–water bath with six 30-s bursts of 200 W with a 30-s interval between bursts, using a Bioruptor (Diagenode). After centrifugation to remove cell debris, chromatin was precleared for 1.5 h at 4°C with a 50% gel slurry of protein A-agarose beads saturated with salmon sperm DNA and bovine serum albumin (Upstate). The precleared chromatin was diluted three times in IP dilution buffer (16.7 mM Tris-Cl [pH 8.1], 167 mM NaCl, 1.2 mM EDTA, 1.1% Triton X-100, 0.01% sodium dodecyl sulfate), and 10% of the supernatants was used as input. The diluted chromatin was incubated overnight on a rotating platform at 4°C with antibodies specific for the proteins of interest. The immune complexes were recovered by a 2-hour incubation at 4°C with a 50% gel slurry of either protein A-agarose or protein-G-agarose beads (Upstate), depending on the antibody specificity. The agarose beads were pelleted and washed twice with 1× dialysis buffer (50 mM Tris-HCl [pH 8.0], 2 mM EDTA, 0.2% Sarkosyl) and sequentially four times with IP wash buffer (100 mM Tris-HCl [pH 9.0], 500 mM LiCl, 1% NP-40, 1% deoxycholic acid). Precipitated chromatin complexes were removed from the beads by incubation with elution buffer (50 mM $NaHCO_3$, 1% sodium dodecyl sulfate) with mild vortexing. This step was repeated, and the eluates were combined. In re-ChIP experiments, immune complexes were eluted by incubation for 30 min at 37°C in 10 mM dithiothreitol. After centrifugation, the supernatant was diluted 25 times with re-ChIP buffer (1% Triton X-100, 2 mM EDTA, 150 mM NaCl, 20 mM Tris-HCl [pH 8.1]) and subjected again to the ChIP procedure using a different antibody. All buffers were supplemented with 1× protease inhibitor cocktail (Complete minus EDTA; Roche). Cross-linking was reversed by adding NaCl to a final concentration of 0.3 M and incubating overnight at 65°C in the presence of RNase A. Samples were then digested with proteinase K at 45°C for 1.5 h. DNA was purified by chromatography on QIAquick columns (QIAGEN) and eluted in double-distilled water, and an aliquot was used for analysis by PCR. Antibodies used in ChIP assays were AcK14-H3 (Upstate; catalog no. 07-353), AcK16-H4 (Upstate; catalog no. 07-329), AcK9-H3 (Upstate; catalog no. 07-352), AHR (Biomol; catalog no. Sa-210), ARNT (Upstate; catalog no. 05-704), DNMT1 (Active motif; catalog no. 39204), HDAC1 (Upstate; catalog no. 05-614), Me2K4-H3 (Abcam; catalog no. ab7766), Me2K9-H3 (Upstate; catalog no. 05-685), Me3K27-H3 (Upstate; catalog no. 07-449), Me3K4-H3 (Abcam; catalog no. ab8580), Me3K9-H3 (Upstate; catalog no. 07-442), MeK27-H3, (Upstate; catalog no. 07-448), MeK9-H3 (Upstate; catalog no. 07-450), p300 (Upstate; catalog no. 05-257), PS10-H3 (Upstate; catalog no. 05-817), and RNA polymerase II (Upstate; catalog no. 05-623). Primers specific for mouse *Cyp1a1*, *Aldh3a1*, and *Nqo1* promoters used to amplify ChIP-purified DNA are indicated in Table 1. Standard end point and real-time PCRs were performed using primers specific for complete coverage of the region between kbp −4.0 and +0.2 of the mouse *Cyp1a1* promoter. The end point PCR products were separated by electrophoresis through 15% polyacrylamide gels and visualized after staining with ethidium bromide.

QRT-PCR analysis. QRT-PCR was performed at least in duplicate in a reaction mixture containing 1× Power SYBR Green PCR master mix (Applied Biosystem), and 0.1 μM of each primer. Amplification was performed on an ABI 7500 real-time PCR system (Applied Biosystems), where the reaction mixture was heated to 95°C for 10 min and immediately cycled 35 times through a denaturing step at 95°C for 15 s and an annealing-elongation step at 60°C for 60 s. Melting curve analyses were performed after PCR amplification to ensure that a single product with the expected melting curve characteristics was obtained as preliminarily determined during primer tests. For analysis of results, we used the sequence detection software (SDS software version 1.3.1; Applied Biosystems).

Data analyses. Relative differences in QRT-PCR among samples were determined using the $\Delta\Delta C_T$ method as described in the Applied Biosytems instructions. The ΔC_T value for each sample was determined using the cycle threshold (C_T) value (obtained from the means of replicates) from the input DNA, to normalize ChIP assay results, or the β-actin signal, to normalize gene expression assays. The $\Delta\Delta C_T$ was calculated by subtracting control ΔC_T values from the corresponding experimental ΔC_T. The resulting values were converted to fold changes over control by raising 2 to the power of $-\Delta\Delta C_T$. For statistical analysis of data, group comparisons were made by one-way analysis of variance. A P value of less than 0.05 was considered statistically significant.

RESULTS

Chromium cross-links HDAC1-DNMT1 complexes to chromatin. Intracellular reduction of Cr(VI) to Cr(III) leads to the formation of Cr-DNA complexes, including DNA-chromium adducts and DNA-DNA and DNA-protein cross-links (56), raising the possibility that transcriptional repression might result from chromium cross-linking HDAC1 to the *Cyp1a1* promoter, disrupting gene induction by B[*a*]P. To test this hypothesis we took advantage of the observation that chelating agents, such as EDTA, disrupt the coordinated bonds of chromium-induced cross-links and dissociate the DNA-DNA and

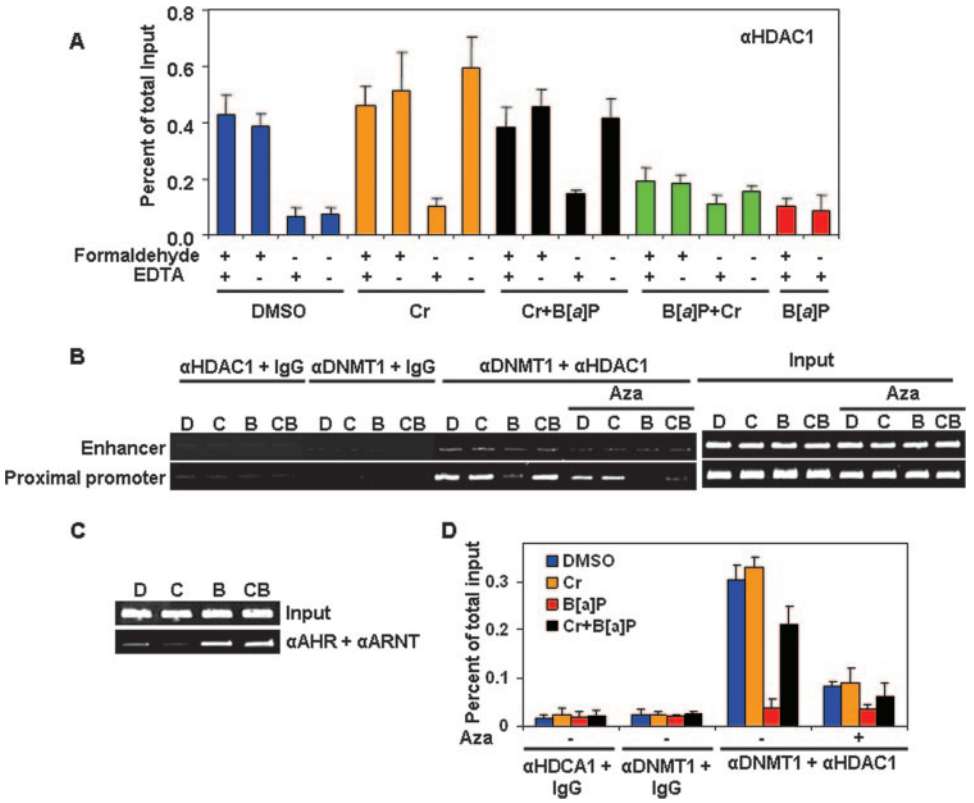

FIG. 1. Chromium cross-links HDAC1 to the *Cyp1a1* promoter and inhibits its B[*a*]P-induced release. Hepa-1 cells were treated for 2 h with DMSO vehicle (D) or 50 μM chromium (Cr and C), for 1.5 h with 5 μM B[*a*]P (B), for 2 h with chromium with 5 μM B[*a*]P for the last 1.5 h (Cr+B[*a*]P and CB), or for 1.5 h with 5 μM B[*a*]P with chromium added for the last hour (B[*a*]P+Cr). (A) ChIP assays were performed as described with specific modifications. For the cross-linking step, cells were incubated with or without formaldehyde, and all subsequent steps were performed the in presence or in the absence of EDTA. HDAC1-immunoprecipitated DNA was amplified by real-time PCR using specific primers spanning the *Cyp1a1* proximal promoter region. Quantification is expressed as percentage of total input, and results are the means (± standard deviations) from three independent experiments. (B) Hepa-1 cells were grown in medium with or without 2 μM Aza for 72 h prior to treatment. Re-ChIP assays were performed by sequential IP with the indicated antibodies. Immunoprecipitated DNA was amplified by real-time PCR using specific primers spanning the *Cyp1a1* proximal promoter region. (C) ReChIP assays were performed on chromatin from cells treated as indicated by sequential IP with antibodies against AHR and ARNT. The DNA was amplified by PCR using specific primers spanning the *Cyp1a1* enhancer region, and PCR products were visualized by ethidium bromide staining after gel electrophoresis. (D) Quantification of the data in panel B is expressed as percentage of total input, and results are the means (± standard deviations) from three independent experiments. All results shown in gels are representative of three independent experiments.

DNA-protein complexes (28, 40, 57). Accordingly, we modified the ChIP protocol to evaluate the possible role of chromium as a cross-linking agent that would substitute for formaldehyde. Chromatin was prepared from Hepa-1 cells exposed to DMSO, chromium, B[*a*]P, and chromium before or after B[*a*]P and incubated with either formaldehyde as a cross-linking agent or with no cross-linking agent. For all subsequent steps of sample manipulation, duplicate buffers were used, containing or not the stipulated concentrations of EDTA. In formaldehyde-cross-linked chromatin, HDAC1 binding was insensitive to EDTA regardless of treatment and was blocked by B[*a*]P treatment when alone or when done prior to chromium (Fig. 1A). Chromium was just as efficient as formaldehyde at retaining HDAC1 bound to chromatin, but unlike with formaldehyde, chromium-mediated binding was sensitive to EDTA, and in all cases EDTA prevented the coimmunoprecipitation of HDAC1 with the *Cyp1a1* promoter (Fig. 1A). Hence, the formation of EDTA-reversible, chromium-induced chromatin-HDAC1 cross-links is likely to be the key process in the mechanism of chromium-induced repression.

The presence of HDAC1 in the uninduced *Cyp1a1* promoter is consistent with the silent status of the gene. HDACs are found in large multiprotein complexes including transcriptional corepressors, such as the silencing mediator for retinoid acid and thyroid hormone receptors, nuclear corepressor, and B-cell lymphoma 6 corepressor (17, 18, 23), and other effectors of epigenetic marks. Among these are the members of the DNMT family of DNA methyltransferases, particularly DNMT1, which play an important role in the epigenetic control of gene expression (11). To determine whether promoter-bound HDAC1 was complexed with DNMT1 on the *Cyp1a1* promoter, we used a ChIP–re-ChIP approach. Chromatin samples were immunoprecipitated with anti-DNMT1, eluted, and, without cross-link reversal, reprecipitated with anti-HDAC1 or with nonspecific IgG antibodies. For analyses, we targeted the proximal promoter region, as defined by the domain bounded between bp −200 and the transcriptional

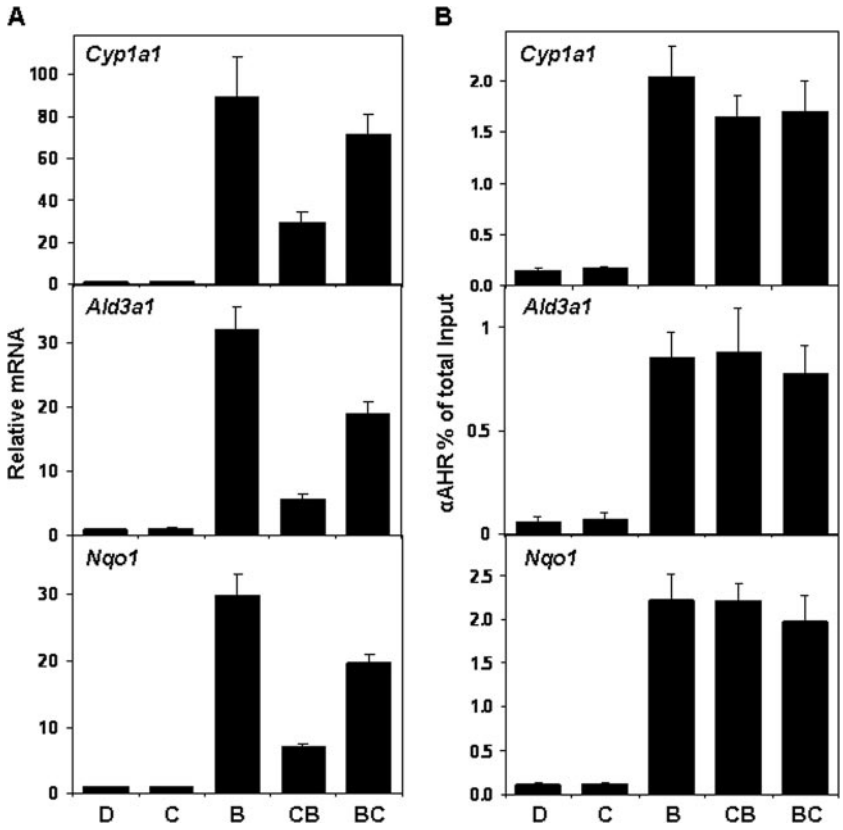

FIG. 2. Chromium inhibits B[*a*]P-inducible gene expression without affecting AHR binding. (A) Hepa-1 cells were treated for 9 h with DMSO (D), 50 μM chromium (C), 50 μM chromium for 1 h followed by 5 μM B[*a*]P for 8 h (CB), or 5 μM B[*a*]P for 8 h with 50 μM chromium added 2 h after B[*a*]P (BC). Total RNA was prepared, and *Cyp1a1*, *Aldh3a1*, and *Nqo1* mRNA expression levels were evaluated by real-time PCR after reverse transcription. Relative mRNA expression is expressed as the induction (*n*-fold) calculated from the ratio of the target signal to β-actin relative to the same ratio in control cells. The data are the means (± standard deviations) from three independent experiments. (B) ChIP assays were performed with anti-AHR antibodies after treatment for 2 h with DMSO (D), 50 μM chromium (C), 5 μM B[*a*]P (B) for 1.5 h, or 50 μM chromium for 0.5 h before (CB) or 1 h after (BC) treatment with 5 μM B[*a*]P for 1.5 h. Immunoprecipitated DNA was amplified and quantified by real-time PCR using specific primers for the *Cyp1a1*, *Aldh3a1*, and *Nqo1* promoter domains containing AHR binding sites. DNA enrichment was normalized to inputs, and data shown are the means ± standard deviations from three independent experiments.

start site, where we showed HDAC1 binding to be maximal (50; M. Schnekenburger and A. Puga, unpublished data). As a positive control, chromatin samples were sequentially immunoprecipitated with anti-AHR followed by anti-ARNT antibodies and PCR amplified for the enhancer region. Sequential IP with anti-DNMT1 followed by anti-HDAC1 antibodies showed that HDAC1 and DNMT1 formed a complex over the proximal promoter chromatin and that this complex was not formed if cells were exposed to B[*a*]P treatment but was retained in chromium-pretreated cells (Fig. 1B). Sequential IP with AHR and ARNT antibodies showed a strong DNA enrichment of the enhancer region in B[*a*]P-treated samples relative to DMSO-treated controls (Fig. 1C). In agreement with previous observations, the interaction of the AHR-ARNT complex with its cognate site remained strong in chromium-pretreated cells. Neither enhancer nor promoter regions were significantly immunoprecipitated by sequential ChIP with nonspecific IgG and anti-DNMT1 or anti-HDAC1. Unexpectedly, cells grown in medium containing Aza, a DNMT1 inhibitor, showed a large decrease in binding of complexes to the *Cyp1a1* promoter (Fig. 1B), suggesting that in the absence of DNMT1, the ability of HDAC1 to bind to the promoter was highly compromised. HDAC1 and DNMT1 protein levels do not change appreciably after any of the treatments in the time frame of these experiments, and hence the ChIP data suggest the establishment of a repressive complex on the proximal promoter domain, with the extent of complex formation and binding depending largely on the presence of DNMT1.

Chromium inhibits RNA polymerase II recruitment. Repression by chromium of AHR-ARNT-dependent induction is not limited to the *Cyp1a1* gene but is a generalized mechanism that extends to *Nqo1* and *Aldh3a1* (Fig. 2A), two other members of the AHR gene battery, and, as determined through global gene expression analyses, to more than 50 other unrelated genes (50). As shown in our previous work (50), repression by chromium is significant only when cells are pretreated with chromium before B[*a*]P treatment and not when B[*a*]P is added first (Fig. 2A), suggesting that the target of chromium repression is an early step, possibly initiation, in transcription. In contrast, regardless of the order of addition, AHR binding is unaffected by chromium exposure (Fig. 2B). To determine the effect of chromium on RNA polymerase II binding, we pretreated cells with chromium, induced *Cyp1a1* with B[*a*]P, and monitored AHR and RNA polymerase II binding to the *Cyp1a1* 5′-flanking sequences by ChIP at 20-min intervals after

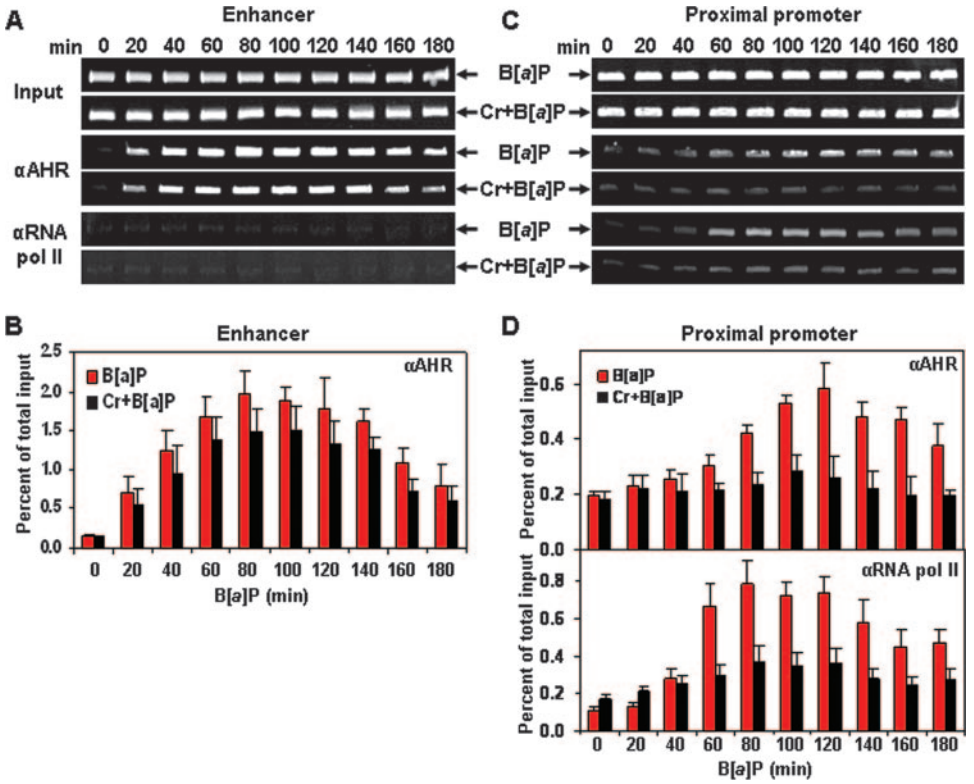

FIG. 3. Chromium blocks B[*a*]P-mediated RNA polymerase II recruitment without affecting the kinetics of AHR binding to the enhancer. Cells were pretreated with 50 μM chromium or with vehicle for 0.5 h, induced with 5 μM B[*a*]P, and subjected to ChIP every 20 min for 3 h with anti-AHR and anti-RNA polymerase II antibodies. (A and C) PCR products resulting from the amplification of the enhancer (kbp −0.8) and the proximal promoter (kbp −0.1) regions (see Fig. 4A for their locations in the *Cyp1a1* promoter), respectively. (B and D) Quantification by real-time PCR, normalized to input DNA, for the AHR binding kinetics to the enhancer (B) and for the binding kinetics of AHR (D, top) and RNA polymerase II (D, bottom) to the proximal promoter. All results are representative of three independent experiments, and quantification data are the means ± standard deviations from three independent experiments.

induction. Neither the time course nor the amount of AHR binding to the enhancer domain (Fig. 3A and B) was significantly affected by chromium treatment, which almost completely inhibited AHR binding to the proximal promoter domain (Fig. 3C and D, top panel). Conversely, RNA polymerase II was recruited to the promoter domain in B[*a*]P-treated cells and not to the enhancer sequences, but, just like the case for the AHR, its association with the proximal promoter was almost completely abolished by chromium (Fig. 3C and D, bottom panel), indicating that repression could be the immediate effect of blocking the AHR-dependent contacts between enhancer and proximal promoter domains and subsequent RNA polymerase II recruitment.

Chromium blocks B[a]P-induced specific chromatin changes necessary for Cyp1a1 expression. To evaluate the effect of chromium on B[*a*]P-induced histone modifications in *Cyp1a1* promoter chromatin, we carried out ChIP analyses with antibodies specific for several histone H3 and H4 modifications known to be involved in gene expression regulation. These included acetylation of Lys-9 and Lys-14 in histone H3 and of Lys-8 and Lys-16 in histone H4, di- and trimethylation at Lys-4 of H3, and phosphorylation at Ser-10 in H3 (42). IPs were performed on chromatin from Hepa-1 cells exposed to DMSO, chromium, B[*a*]P, and chromium added before or after B[*a*]P treatment. These assays were associated with a systematic mapping of the *Cyp1a1* promoter between kb −3.6 and +0.6 from the transcription start site (Fig. 4A) to detect any localized changes that might result from chromium exposure compared to normal changes related to *Cyp1a1* gene transactivation. Acetylation of K16 in histone H4 and of K9 and K14 in histone H3 was strongly induced by B[*a*]P relative to DMSO-treated control cells in the enhancer and proximal promoter regions, respectively, and was considerably inhibited when cells were pretreated with chromium (Fig. 4B and C). Similarly, phosphorylation of S10 in histone H3, which is a significant mark that is increased in the enhancer domain of B[*a*]P-induced cells, was inhibited when cells were exposed to chromium before B[*a*]P treatment (Fig. 4B and C). Addition of a third methyl group to already-dimethylated K4 in histone H3 was also a significant mark of B[*a*]P-dependent gene induction and was abolished when cells were exposed to chromium before B[*a*]P (Fig. 4B and C), but not the reverse. The repressive histone marks of di-and trimethylation at H3 K9 and H3 K27 were absent from the *Cyp1a1* promoter, acetylation of K8 in histone H4 showed no changes with any of the treatments (not shown), and control IPs with nonspecific IgG showed a low overall background level over the entire 5′-flanking region of the *Cyp1a1* gene. Hence, chromium treatment inhibits specific marks associated with gene induction by the B[*a*]P-activated AHR.

HDAC1 siRNA, NaB, and Aza reduce transcriptional repression by chromium. Total HDAC and immunoprecipitable

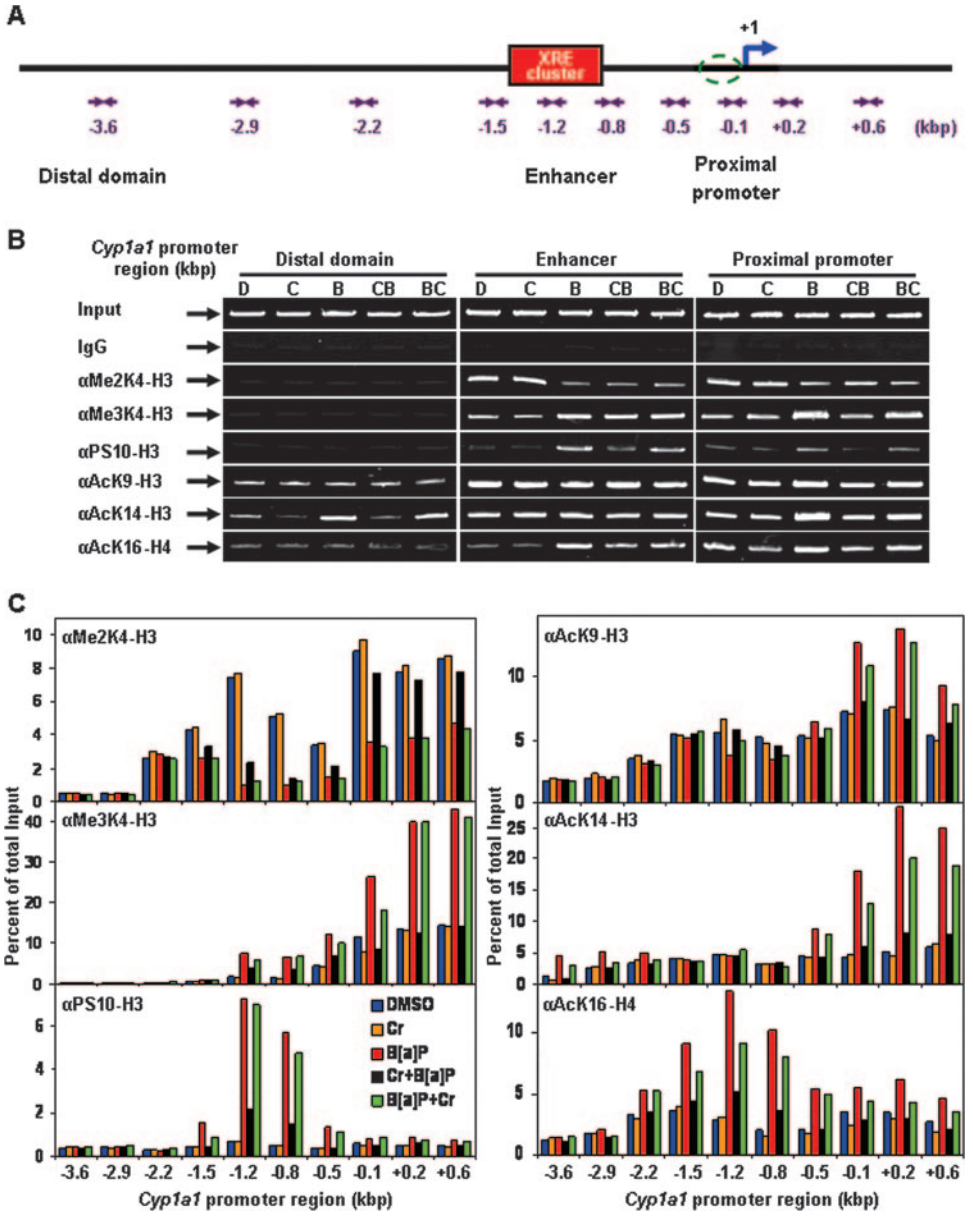

FIG. 4. Chromium inhibits B[*a*]P-induced modification of specific histone amino acids in *Cyp1a1* promoter chromatin. (A) Schematic representation of the mouse *Cyp1a1* promoter from kbp −4.0 to +1.0 with the PCR primer positions used to map the promoter in ChIP experiments. Positions of AhRE motifs and primers (purple arrows) relative to the transcriptional start site (blue arrow, numbered as +1) are indicated. A nucleosome (green dashed circle), probably positioned over the promoter, is localized on the scheme. (B and C) Cells were treated for 2 h with DMSO (D) or 50 μM chromium (Cr or C), for 1.5 h with 5 μM B[*a*]P (B), for 2 h with chromium with 5 μM B[*a*]P for the last 1.5 h, (Cr+B[*a*]P or CB), or for 1.5 h with 5 μM B[*a*]P with chromium added for the last hour (B[*a*]P+Cr or BC). (B) ChIP used the indicated antibodies specific for posttranslationally modified histone amino acids. Real-time PCR products amplified with primers for the distal (kbp −3.2), enhancer (kbp −0.8), and proximal promoter (kbp −0.1) domains were resolved by electrophoresis. (C) Representative results of two or three independent real-time PCR amplification experiments are expressed as percentage of total input.

HDAC1 activities were not affected by chromium treatment (Table 2), suggesting that the transcriptional repression exerted by chromium on *Cyp1a1* gene induction resulted from the irreversible physical presence of promoter-bound HDAC1-DNMT1 complexes and not from their functional inhibition. If the continued presence of HDAC1 plays such a crucial role in chromium repression, we might expect that its removal would relieve transcriptional repression. We tested this hypothesis by

TABLE 2. HDAC activity in chromium-treated Hepa-1 cells

Treatment	HDAC activity (pmol · min^{-1} · mg^{-1} protein)		
	Total	Anti-HDAC1 IP	Nonimmune IgG IP
DMSO	1,420 ± 80	6.6 ± 0.4	0.1 ± 0.03
Cr	1,530 ± 70	6.6 ± 0.7	0.1 ± 0.05
B[*a*]P	1,440 ± 10	6.9 ± 0.4	0.1 ± 0.06
Cr + B[*a*]P	1,570 ± 70	6.8 ± 0.6	0.1 ± 0.02

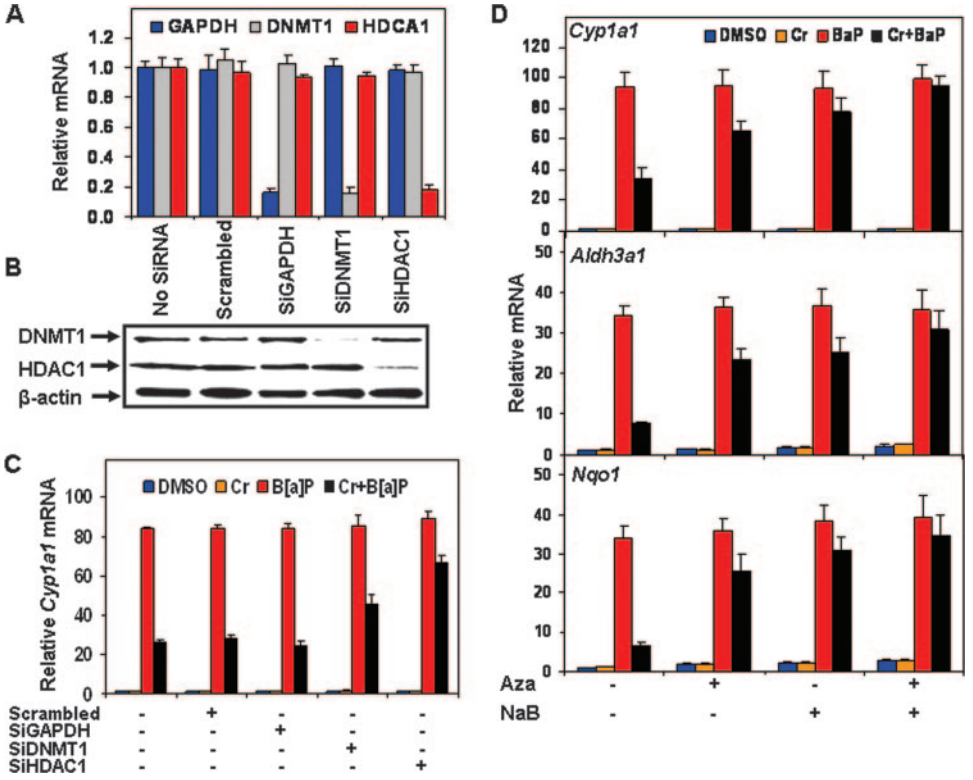

FIG. 5. HDAC1 siRNA, NaB, and Aza block chromium-induced transcriptional repression of B[*a*]P-inducible *Cyp1a1* expression. Cells were transfected with GAPDH siRNA, scrambled siRNA, DNMT1 siRNA, HDAC1 siRNA, or no siRNA. (A to C) At 48 h posttransfection, the effect of the siRNAs on target gene expression was evaluated for mRNA (A) and protein levels (B), or the cells were treated with DMSO, 50 μM chromium for 9 h, 5 μM B[*a*]P for 8 h, or 50 μM chromium for 1 h followed by 5 μM B[*a*]P for an additional 8 h. *Cyp1a1* mRNA expression was determined in these samples by real-time PCR (C). Relative mRNA expression is expressed as induction (*n*-fold) calculated as the ratio of target signal to β-actin relative to the same ratio in the control cells. (D) Hepa-1 cells were maintained in a medium with or without 2 μM Aza for 72 h, 2 mM NaB for 16 h, or both and treated with chromium or B[*a*]P as for panel C. Total RNA was extracted, and *Cyp1a1*, *Aldh3a1*, and *Nqo1* mRNA expression levels were determined by real-time PCR after reverse transcription. Relative mRNA expression is expressed as the induction (*n*-fold) calculated from the ratio of the target signal to β-actin relative to the same ratio in control cells. The data are the means (± standard deviations) from three independent experiments.

knocking down HDAC1 expression using transient transfection of HDAC1 siRNA oligonucleotides. Control experiments at 48 h posttransfection showed that the mRNA (Fig. 5A) and protein (Fig. 5B) levels of *Hdac1* and *Gapdh* were reduced to less than 10% of the levels in control cells in cells transfected by their respective siRNA oligonucleotides but not by a scrambled oligonucleotide control. HDAC1 knockdown with two different siRNAs, but not GAPDH knockdown, caused the near-complete inhibition of the chromium-mediated transcriptional repression of *Cyp1a1* (Fig. 5C). Basal and B[*a*]P-induced *Cyp1a1* mRNA levels remained unchanged following HDAC1 depletion relative to controls, indicating that transactivation of the gene was not impaired by transfection of HDAC1 siRNA oligonucleotides and that, in addition to HDAC1 removal, further chromatin modifications associated with AHR complex binding were needed for transcription initiation.

Irreversibly bound HDAC1 could inhibit transcription by sterically hindering binding of basal transcriptional complexes or, alternatively, by maintaining a constant state of deacetylation of histone residues, such as H3-K9 and H3-K14, needed to be acetylated for B[*a*]P-induced transcription to proceed. To distinguish between these two possibilities, we investigated the effect of HDAC and DNMT inhibitors, NaB and Aza, respectively, on chromium-mediated repression. We compared constitutive and induced mRNA levels of three AHR battery genes, *Cyp1a1*, *Aldh3a1*, and *Nqo1* in cells cultured with or without Aza, NaB, or both. Neither Aza nor NaB changed the level of constitutive or B[*a*]P-induced mRNA expression of these three genes (Fig. 5D), yet repression by chromium was blocked by either inhibitor and was almost completely abolished when the two inhibitors were combined (Fig. 5D).

To measure the effect of the inhibitors on HDAC1 and DNMT1 binding to the enhancer and the proximal promoter *Cyp1a1* domains, chromatin from cells grown in the presence of either inhibitor and treated with DMSO, chromium, B[*a*]P, or chromium plus B[*a*]P was immunoprecipitated with anti-HDAC1, anti-DNMT1, anti-AHR, and anti-p300 antibodies. Aza and NaB treatments decreased the interaction of HDAC1 and DNMT1 with the *Cyp1a1* promoter by only 40 to 60% in either enhancer or proximal promoter sequences (Fig. 6A and B), significantly less than their inhibitory effect on repression. Neither treatment affected B[*a*]P-dependent AHR recruitment to its cognate sequences in the enhancer or proximal promoter domains or promoted recruitment of p300 to either domain (Fig. 6A and B).

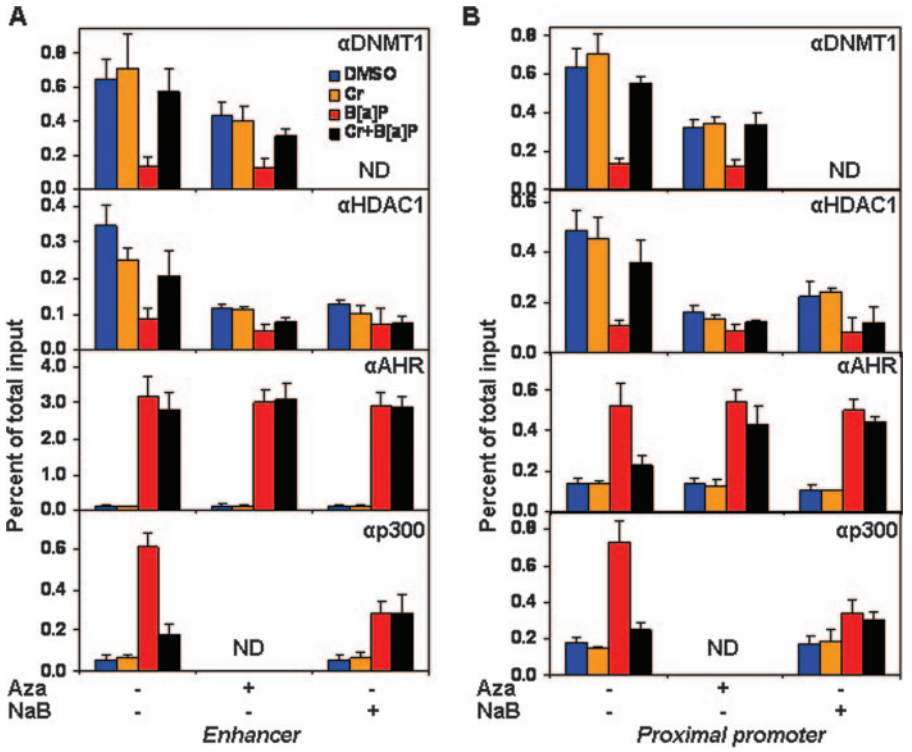

FIG. 6. NaB and Aza partially reduce occupancy of the *Cyp1a1* promoter by HDAC1 and DNMT1 but do not recruit AHR and p300. Hepa-1 cells were maintained in medium with or without 2 μM Aza for 72 h, 2 mM NaB for 16 h, or a combination of both agents. Cells were treated for 2 h with DMSO, 50 μM chromium, 5 μM B[*a*]P, or 50 μM chromium for 0.5 h followed by 5 μM B[*a*]P for an additional 1.5 h. ChIP assays used HDAC1, DNMT1, AHR, and p300 antibodies. DNA enrichment was quantified by real-time PCR and expressed as percentage of total input. Data are the means (± standard deviations) from three independent experiments. ND, not done.

Aza and NaB reverse the inhibition of histone marks induced by chromium. The data presented so far are consistent with the concept that, by blocking release of HDAC1-DNMT1, chromium forces the *Cyp1a1* promoter into a state of permanent histone deacetylation, preventing B[*a*]P-induced specific histone modifications involved in chromatin remodeling necessary for *Cyp1a1* gene expression. If this was the case, it would be expected that inhibition of HDAC1 or DNMT1 would reverse the effect of chromium and allow for the critical acetylation events associated with transcriptional induction. To test this prediction, we investigated whether Aza and NaB treatments would have an effect on the modification of those critical histone marks. Chromatin from cells cultured with or without Aza, NaB, or both and then treated with DMSO, chromium, B[*a*]P, or chromium followed by B[*a*]P was immunoprecipitated with antibodies specific for the histone H3 and H4 modifications previously determined to be inhibited by chromium (Fig. 4), including AcK14-H3, AcK16-H4, Me2K4-H3, Me3K4-H3, and pS10-H3, as well as with anti-AHR antibodies. Specific enrichment of immunoprecipitated DNA was evaluated by QRT-PCR with specific primers for enhancer and proximal *Cyp1a1* promoter domains. Neither Aza nor NaB changed the constitutive or B[*a*]P-induced levels of AHR binding to the enhancer domain, which, as already shown, were unaffected by chromium (Fig. 7A). The chromium-induced repression of B[*a*]P-dependent AHR recruitment to the proximal promoter was, however, blocked in cells pretreated with either inhibitor and was completely abolished when the inhibitors were combined (Fig. 7B). In contrast, Aza and NaB treatments induced a 5- to 10-fold increase in the constitutive acetylation levels of K14-H3 in the proximal promoter and of K16-H4 in the enhancer, restoring, in chromium-treated cells, the acetylation levels found in B[*a*]P-induced cells (Fig. 7A and B). The inhibitors also had a strong effect on the phosphorylation and methylation marks in the enhancer and proximal promoter, respectively (Fig. 7A and B), reversing as well the chromium-dependent repression of both phosphorylation of S10-H3 in the enhancer and the addition of a third methyl group to already-dimethylated K4-H3 in the proximal promoter.

Chromium pretreatment enhances the formation of stable BPDE-DNA adducts. The monooxygenase activity of the cytochrome P450 CYP1A1 is the major B[*a*]P-metabolizing enzyme in the liver, responsible for the activation and detoxification of highly reactive diol epoxides that form mutagenic adducts with DNA (33). We asked whether *Cyp1a1* repression by chromium had an impact on B[*a*]P metabolism by examining the formation of bulky DNA adducts after treatment of cells with B[*a*]P alone or preceded for 30 min by increasing concentrations of chromium. Treatment with 1.0 μM B[*a*]P generated a single major adduct with a chromatographic migration pattern consistent with that of BPDE adducted to guanine. Adduct yields in the absence of chromium were statistically indistinguishable from background but were significantly increased by chromium pretreatment. Cells preexposed to 25 μM chromate prior to 1 μM B[*a*]P showed a 15-fold

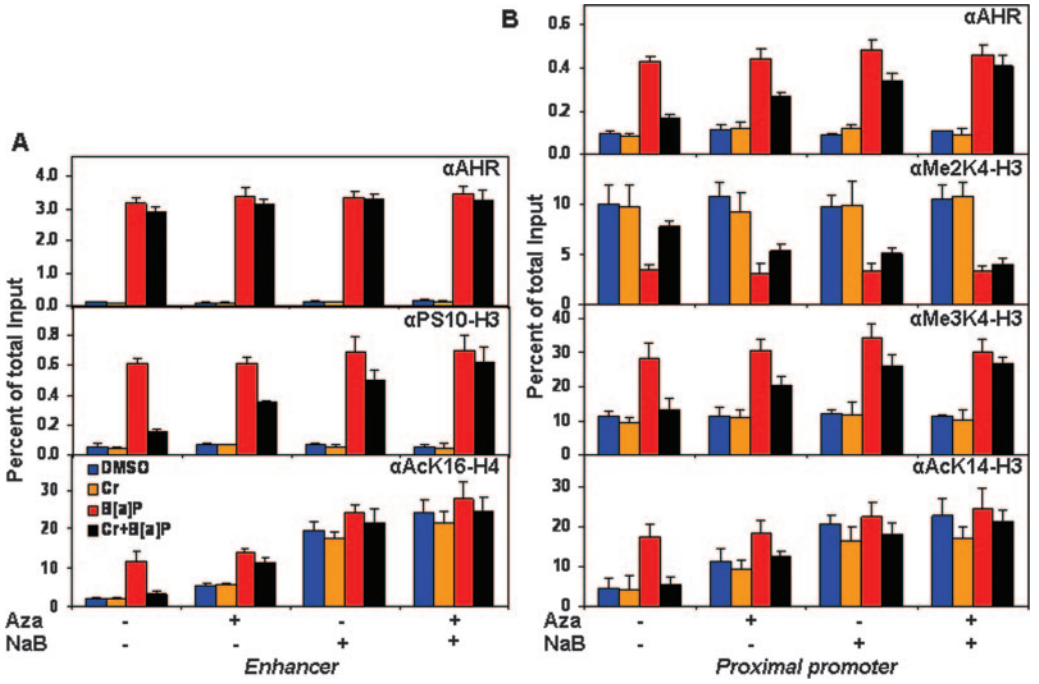

FIG. 7. NaB and Aza reverse the inhibition of histone modifications induced by chromium. Hepa-1 cells were maintained in medium with or without 2 μM Aza for 72 h, 2 mM NaB for 16 h, or a combination of both agents and were treated for 2 h with DMSO, 50 μM chromium, 5 μM B[*a*]P for 1.5 h, or 50 μM chromium for 0.5 h followed by 5 μM B[*a*]P for an additional 1.5 h. ChIP assays were performed with the indicated antibodies raised against the specific posttranslational histone modifications indicated in the graphs. Immunoprecipitated DNA was amplified by real-time PCR using primers specific for the indicated enhancer and proximal promoter regions. DNA enrichment is expressed as percentage of the total input. Results are the means ± standard deviations from two independent experiments.

adduct increase over control levels at the 2-hour point, and cell showed a 4-fold increase at the 24-hour point when pretreated with 1 μM chromate (Fig. 8). This pattern of higher adduct yield with increasing chromium exposure may have major biological consequences in regard to the mutagenicity and carcinogenicity of mixtures of these environmental agents.

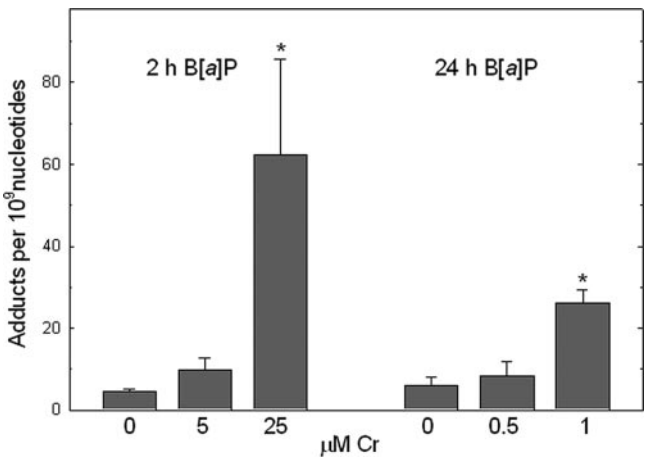

FIG. 8. Formation of BPDE-DNA adducts is dose dependent and is potentiated by chromium pretreatment. Hepa-1 cells were pretreated with the indicated concentration of sodium chromate for 30 min before addition of 1 μM B[*a*]P to the culture medium. Cells were harvested for adduct determination after 2 h and 24 h of B[*a*]P treatment. The total adduct level is shown as the number of adducts per 10^9 nucleotides. Each bar represents the mean ± standard error from two independent experiments. The asterisks denote statistical significance ($P < 0.05$) for the comparison of chromium pretreatment to DMSO treatment for the same length of B[*a*]P treatment.

DISCUSSION

In this article we describe experiments addressing the mechanisms responsible for chromium-mediated transcriptional repression of the *Cyp1a1* gene. We find that the critical repressive event is the formation of coordinated HDAC1-DNMT1-chromium-chromatin complexes in the proximal promoter that impair recruitment of the basal transcriptional complex, including RNA polymerase II and p300. The complexes block acetylation of critical histone residues associated with AHR-mediated transactivation but allow the formation of activated AHR complexes in the enhancer domain to proceed unimpeded, underscoring the fact that AHR activation, although necessary, is not sufficient to up-regulate transcription of its target genes. As shown here, the *Cyp1a1* gene, other genes in the AHR gene battery, and possibly some 50 other B[*a*]P-inducible genes (50) become silenced in this manner.

The intracellular reduction of Cr(VI), which happens very quickly in both the cytoplasm and nuclei of treated cells (50), results in formation of Cr(III) through the transient intracellular formation of highly reactive intermediate oxidation states (56). Growing evidence suggests that the primary event in the disruption of gene expression and cellular functions by Cr(VI) is the formation of nuclear Cr(III)-DNA complexes (36, 39), one of which, we show, is the cross-linked (or coordinated) complex between HDAC1 and chromatin, which is sensitive to chelating agent disruption. It is likely that other Cr(III)-medi-

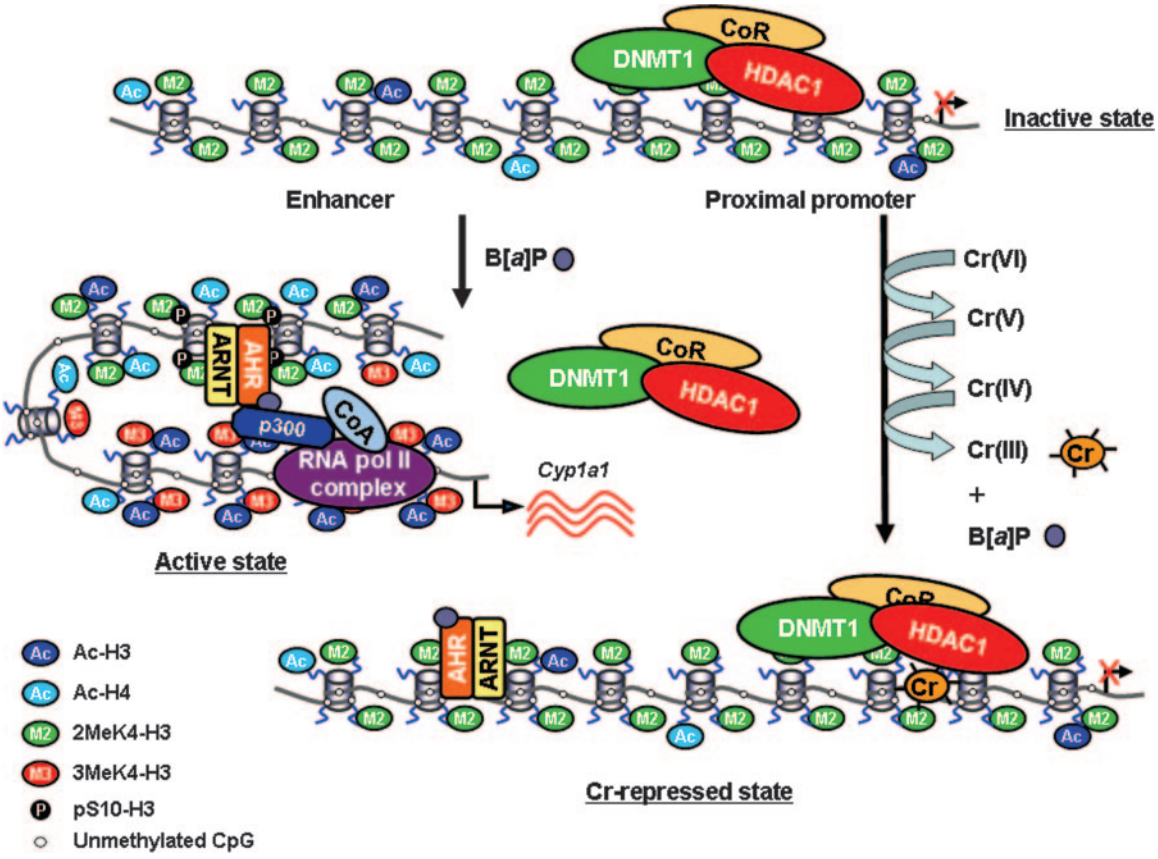

FIG. 9. Schematic model of chromium-induced transcriptional repression. This model summarizes results reported here and in previous reports (25, 50). In the inactive state, *Cyp1a1* is silent due to the presence of the complexes formed by DNMT1 and HDAC1, the hypoacetylation of histone tails, and a high level of dimethylated Lys4-H3. AHR activation by a ligand, such as B[*a*]P, causes ligand-activated AHR-ARNT complexes (represented here by a single heterodimer) to bind to the cognate AhREs in the enhancer region. Binding of the AHR-ARNT complex promotes an active state characterized by the phosphorylation of Ser10-H3 in the enhancer region, trimethylation of Lys4-H3 in the proximal promoter, and hyperacetylation of histone tails across the promoter. Here shown as a chromatin-bending loop, but possibly also the result of sliding, the enhancer complex makes contact with the proximal promoter; releases the repressive HDAC1-DNMT1 complexes; allows recruitment of coactivators, general transcription factors, and the RNA polymerase II complex; and initiates *Cyp1a1 trans*-activation. Preexposure to Cr(VI), rapidly reduced to Cr(III), causes cross-linking (coordination) of HDAC1-DNMT1 complexes to the promoter, maintaining a chronic state of histone deacetylation that inhibits recruitment of p300 and the AHR complex to the proximal promoter and establishing a chromium-repressed state.

ated complexes for which there is no current assay may be formed as well.

Not surprisingly, the HDAC1 complex includes DNMT1, and in fact it is the HDAC1-DNMT1 complexes that are cross-linked to chromatin. Depletion of DNMT1 by Aza treatment prevents formation of these complexes, which agrees with results from several studies reporting that inhibitors of HDAC and DNMT decrease the interaction of those proteins with their targets (12, 13, 55). Following conversion to the nucleoside triphosphate, Aza is incorporated into DNA instead of dCTP during replication, inhibiting DNA methylation by DNMTs probably through formation of a covalent complex between DNA-incorporated Aza and DNMT1 that sequesters the functional enzyme (41). Hence, sequestration away from HDAC1 has the ultimate effect of blocking formation of the complex. It is worth noting that recruitment of DNMT1 does not lead to methylation of a canonical CpG island in the *Cyp1a1* gene (M. Schnekenburger, L. Peng, and A. Puga, unpublished data).

Although the AHR complex binds unimpeded to the enhancer domain, its recruitment to the proximal promoter, which is evident in B[*a*]P-treated cells, is blocked by chromium, and so is recruitment of RNA polymerase II. It has been proposed (46) that AHR-ARNT-mediated *Cyp1a1* transcriptional activation takes place by a looping mechanism whereby the AHR complex bends chromatin to make contact with the basal transcriptional machinery being assembled at the proximal promoter. Whether a looping or a simpler sliding mechanism is correct, our data indicate that chromium blocks the contact between the enhanceosome and basal transcription complexes involved in rapid recruitment of the transcriptional machinery to the *Cyp1a1* gene. Previous reports have described the presence of a nucleosome poised over the proximal promoter region, blocking transcription initiation (31). Given the localization, it is likely that the repressive HDAC1-DNMT1 complex is constitutively associated with this nucleosome and that, under normal induction conditions, it is released by B[*a*]P treatment, but it becomes cross-linked by chromium, thus preventing nucleosome removal, RNA polymerase II recruitment, and transcription initiation.

Chromium treatment does not lead to overall loss of HDAC activity. As a consequence, retention of chromatin-bound HDAC1 causes the deacetylation of histone marks associated with gene activation by B[*a*]P treatment, such as AcK9-H3, AcK14-H3, and AcK16-H4 (30); phosphorylation of S10-H3; and addition of a third methyl group to dimethylated K4-H3, which is a mark found exclusively associated with active genes (42). HDAC and DNMT inhibitors or HDAC1 knockdown, even though they have no ulterior effect on constitutive or B[*a*]P-induced levels of *Cyp1a1* expression, restore acetylation marks, block chromium repression, and allow inducible transcription. Concomitantly, all other histone marks induced by B[*a*]P and blocked by chromium, including phosphorylation and methylation marks not directly related to acetylation, are reversed, suggesting that the acetylation marks are the key gatekeepers that must happen first for the other modifications to occur.

B[*a*]P is metabolized into BPDE, the ultimate carcinogen, by the cytochrome P450 enzymes CYP1A1 and CYP1B1. Repression of *Cyp1a1* expression will create a state of increased toxicant load, a high level of BPDE-DNA adducts with the inability to respond by induction of the appropriate detoxification pathway. Studies with *Cyp1a1* knockout mice have shown that lack of CYP1A1 enzymatic activity leads to a large increase of BPDE-DNA adducts in liver. In mice, this state is followed by wasting immunosuppression and premature death (47–49). CYP1A1, however, is practically the only B[a]P-metabolizing P450 expressed in Hepa-1 cells, and it would be expected that its repression would decrease, rather than increase, the formation of BPDE adducts. This might be due to repression of phase II genes, which, as suggested by the data in Fig. 2A, may be even more pronounced than repression of *Cyp1a1*.

The main features of our findings as described above are schematically represented in the model shown in Fig. 9, showing the inducible conversion of an inactive to an active AHR transcriptional complex by exposure to the ligand, B[*a*]P, or its conversion to a repressed complex by the presence of ligand and exposure to one or another of several highly reactive chromium intermediate oxidation states.

Down-regulation of gene expression by chromium is not unique to genes regulated by the AHR. A large amount of evidence suggests that chromium does not affect constitutive gene expression but interferes with an early step of gene induction (1, 26, 29, 37, 44, 50, 52). Our observations strongly point at the possibility that epigenetic mechanisms of gene regulation might be a central target of chromium toxicity and that inhibition of these mechanisms reduces the capacity of cells to respond to environmental hazards. Long-term exposure to chromium, by inducing a chronic cross-linking of inhibitory complexes may cause a significant increase in histone deacetylation, which would lead to histone methylation in specific positions involved in gene repression and silencing and to subsequent DNA hypermethylation, which would soon be converted into a complete and efficient state of gene silencing. Such changes could cause epigenetic and structural alterations leading to changes in gene transcription and ultimately, if occurring at critical cell cycle regulatory genes, to chromium-mediated transformation and carcinogenesis. These observations raise the possibility that chromium exposure during development may also modify developmental imprinting patterns and be related to transgenerational carcinogenesis. Consistent with this prediction, paternal exposure to chromium prior to mating was found to alter the incidence of neoplastic and nonneoplastic changes in mouse tissues of the offspring (6). In this context, regulation of the $p16^{ink4a}$ tumor suppressor gene appears to be a major target of chromium toxicity. Cigarette smoking is a major source of coexposure to chromium and B[*a*]P, and several studies have reported the association between aberrant p16 methylation and smoking (20, 22). Hypermethylation of the $p16^{ink4a}$ promoter has also been found in one-third of chromate workers with a history of exposure for 15 years or more who developed lung cancer (24).

In addition to being a powerful carcinogen, hexavalent chromium is embryotoxic, causes birth defects in wildlife and laboratory animals (35), and has been epidemiologically associated with birth defects in humans (15). During embryonic stem cell differentiation and in differentiated cells, developmental genes are held in a "transcription-ready" state (38) mediated by a "bivalent" promoter chromatin pattern consisting of the repressive mark, histone H3 methylated at Lys27 by Polycomb group proteins, plus the active mark, histone H3 methylated at Lys4 by the Trithorax proteins (3). Our observation that B[*a*]P treatment strongly induces H3-Lys4 trimethylation and that chromium inhibits this methylation opens up the interesting possibility that combined exposure during development to binary mixtures of B[*a*]P and chromium, or to the single compounds, may derail developmental imprinting patterns.

ACKNOWLEDGMENTS

We thank Ying Xia for critical reading of the manuscript and Yunxia Fan and Brenda L. Schumann for expert technical assistance.

This research was supported by NIEHS grants R01 ES06273 and R01 ES10807, NIEHS Center for Environmental Genetics grant P30 ES06096, and NIEHS Superfund Basic Research Program grant P42 ES04908.

REFERENCES

1. **Alcedo, J. A., M. Misra, J. W. Hamilton, and K. E. Wetterhahn.** 1994. The genotoxic carcinogen chromium(VI) alters the metal-inducible expression but not the basal expression of the metallothionein gene in vivo. Carcinogenesis **15:**1089–1092.
2. **Barchowsky, A., and K. A. O'Hara.** 2003. Metal-induced cell signaling and gene activation in lung diseases. Free Radic. Biol. Med. **34:**1130–1135.
3. **Bernstein, B. E., T. S. Mikkelsen, X. Xie, M. Kamal, D. J. Huebert, J. Cuff, B. Fry, A. Meissner, M. Wernig, K. Plath, R. Jaenisch, A. Wagschal, R. Feil, S. L. Schreiber, and E. S. Lander.** 2006. A bivalent chromatin structure marks key developmental genes in embryonic stem cells. Cell **125:**315–326.
4. **Brylawski, B. P., G. J. Tsongalis, M. Cordeiro-Stone, W. T. May, L. D. Comeau, and D. G. Kaufman.** 1993. Association of putative origins of replication with the nuclear matrix in normal human fibroblasts. Cancer Res. **53:**3865–3868.
5. **Cefalu, W. T., Z. Q. Wang, X. H. Zhang, L. C. Baldor, and J. C. Russell.** 2002. Oral chromium picolinate improves carbohydrate and lipid metabolism and enhances skeletal muscle Glut-4 translocation in obese, hyperinsulinemic (JCR-LA corpulent) rats. J. Nutr. **132:**1107–1114.
6. **Cheng, R. Y., T. Hockman, E. Crawford, L. M. Anderson, and Y. H. Shiao.** 2004. Epigenetic and gene expression changes related to transgenerational carcinogenesis. Mol. Carcinog. **40:**1–11.
7. **Cheu, J., G. Talaska, M. Miller, C. Rice, and D. Warshawsky.** 1997. Benzo-[a]pyrene coated ferric oxide and aluminum oxide particles: uptake, metabolism and DNA binding in hamster pulmonary alveolar macrophages and tracheal epithelial cells in vitro. Carcinogenesis **18:**167–175.
8. **Dayan, A. D., and A. J. Paine.** 2001. Mechanisms of chromium toxicity, carcinogenicity and allergenicity: review of the literature from 1985 to 2000. Hum. Exp. Toxicol. **20:**439–451.
9. **Ding, M., X. Shi, V. Castranova, and V. Vallyathan.** 2000. Predisposing factors in occupational lung cancer: inorganic minerals and chromium. J. Environ. Pathol. Toxicol. Oncol. **19:**129–138.
10. **Dipple, A.** 1995. DNA adducts of chemical carcinogens. Carcinogenesis **16:**437–441.
11. **El-Osta, A., P. Kantharidis, J. R. Zalcberg, and A. P. Wolffe.** 2002. Precip-

itous release of methyl-CpG binding protein 2 and histone deacetylase 1 from the methylated human multidrug resistance gene (*MDR1*) on activation. Mol. Cell. Biol. **22:**1844–1857.
12. **Ghoshal, K., J. Datta, S. Majumder, S. Bai, X. Dong, M. Parthun, and S. T. Jacob.** 2002. Inhibitors of histone deacetylase and DNA methyltransferase synergistically activate the methylated metallothionein I promoter by activating the transcription factor MTF-1 and forming an open chromatin structure. Mol. Cell. Biol. **22:**8302–8319.
13. **Gialitakis, M., A. Kretsovali, C. Spilianakis, L. Kravariti, J. Mages, R. Hoffmann, A. K. Hatzopoulos, and J. Papamatheakis.** 2006. Coordinated changes of histone modifications and HDAC mobilization regulate the induction of MHC class II genes by Trichostatin A. Nucleic Acids Res. **34:** 765–772.
14. **Gibb, H. J., P. S. Lees, P. F. Pinsky, and B. C. Rooney.** 2000. Lung cancer among workers in chromium chemical production. Am. J. Ind. Med. **38:**115–126.
15. **Goldberg, S. J., M. D. Lebowitz, E. J. Graver, and S. Hicks.** 1990. An association of human congenital cardiac malformations and drinking water contaminants. J. Am. Coll. Cardiol. **16:**155–164.
16. **Hankinson, O.** 1995. The aryl hydrocarbon receptor complex. Annu. Rev. Pharmacol. Toxicol. **35:**307–340.
17. **Huang, E. Y., J. Zhang, E. A. Miska, M. G. Guenther, T. Kouzarides, and M. A. Lazar.** 2000. Nuclear receptor corepressors partner with class II histone deacetylases in a Sin3-independent repression pathway. Genes Dev. **14:**45–54.
18. **Huynh, K. D., W. Fischle, E. Verdin, and V. J. Bardwell.** 2000. BCoR, a novel corepressor involved in BCL-6 repression. Genes Dev. **14:**1810–1823.
19. **Ikuta, T., H. Eguchi, T. Tachibana, Y. Yoneda, and K. Kawajiri.** 1998. Nuclear localization and export signals of the human aryl hydrocarbon receptor. J. Biol. Chem. **273:**2895–2904.
20. **Jarmalaite, S., A. Kannio, S. Anttila, J. R. Lazutka, and K. Husgafvel-Pursiainen.** 2003. Aberrant p16 promoter methylation in smokers and former smokers with nonsmall cell lung cancer. Int. J. Cancer **106:**913–918.
21. **Kazlauskas, A., S. Sundstrom, L. Poellinger, and I. Pongratz.** 2001. The hsp90 chaperone complex regulates intracellular localization of the dioxin receptor. Mol. Cell. Biol. **21:**2594–2607.
22. **Kim, D. H., H. H. Nelson, J. K. Wiencke, S. Zheng, D. C. Christiani, J. C. Wain, E. J. Mark, and K. T. Kelsey.** 2001. p16(INK4a) and histology-specific methylation of CpG islands by exposure to tobacco smoke in non-small cell lung cancer. Cancer Res. **61:**3419–3424.
23. **Ko, H. P., S. T. Okino, Q. Ma, and J. P. Whitlock, Jr.** 1996. Dioxin-induced CYP1A1 transcription in vivo: the aromatic hydrocarbon receptor mediates transactivation, enhancer-promoter communication, and changes in chromatin structure. Mol. Cell. Biol. **16:**430–436.
24. **Kondo, K., Y. Takahashi, Y. Hirose, T. Nagao, M. Tsuyuguchi, M. Hashimoto, A. Ochiai, Y. Monden, and A. Tangoku.** 2006. The reduced expression and aberrant methylation of p16(INK4a) in chromate workers with lung cancer. Lung Cancer **53:**295–302.
25. **Maier, A., T. P. Dalton, and A. Puga.** 2000. Disruption of dioxin-inducible phase I and phase II gene expression patterns by cadmium, chromium, and arsenic. Mol. Carcinog. **28:**225–235.
26. **Majumder, S., K. Ghoshal, D. Summers, S. Bai, J. Datta, and S. T. Jacob.** 2003. Chromium(VI) down-regulates heavy metal-induced metallothionein gene transcription by modifying transactivation potential of the key transcription factor, metal-responsive transcription factor 1. J. Biol. Chem. **278:** 26216–26226.
27. **Manning, F. C., J. Xu, and S. R. Patierno.** 1992. Transcriptional inhibition by carcinogenic chromate: relationship to DNA damage. Mol. Carcinog. **6:**270–279.
28. **Mattagajasingh, S. N., and H. P. Misra.** 1999. Analysis of EDTA-chelatable proteins from DNA-protein crosslinks induced by a carcinogenic chromium(VI) in cultured intact human cells. Mol. Cell. Biochem. **199:**149–162.
29. **McCaffrey, J., C. M. Wolf, and J. W. Hamilton.** 1994. Effects of the genotoxic carcinogen chromium(VI) on basal and hormone-inducible phosphoenolpyruvate carboxykinase gene expression in vivo: correlation with glucocorticoid- and developmentally regulated expression. Mol. Carcinog. **10:**189–198.
30. **McGarvey, K. M., J. A. Fahrner, E. Greene, J. Martens, T. Jenuwein, and S. B. Baylin.** 2006. Silenced tumor suppressor genes reactivated by DNA demethylation do not return to a fully euchromatic chromatin state. Cancer Res. **66:**3541–3549.
31. **Morgan, J. E., and J. P. Whitlock, Jr.** 1992. Transcription-dependent and transcription-independent nucleosome disruption induced by dioxin. Proc. Natl. Acad. Sci. USA **89:**11622–11626.
32. **Muller, M. M., E. Schreiber, W. Schaffner, and P. Matthias.** 1989. Rapid test for in vivo stability and DNA binding of mutated octamer binding proteins with 'mini-extracts' prepared from transfected cells. Nucleic Acids Res. **17:** 6420.
33. **Nebert, D. W., and H. V. Gelboin.** 1968. Substrate-inducible microsomal aryl hydroxylase in mammalian cell culture. I. Assay and properties of induced enzyme. J. Biol. Chem. **243:**6242–6249.
34. **Nebert, D. W., A. L. Roe, M. Z. Dieter, W. A. Solis, Y. Yang, and T. P. Dalton.** 2000. Role of the aromatic hydrocarbon receptor and [Ah] gene battery in the oxidative stress response, cell cycle control, and apoptosis. Biochem. Pharmacol. **59:**65–85.
35. **Nguyen, L. T., and C. R. Janssen.** 2001. Comparative sensitivity of embryo-larval toxicity assays with African catfish (Clarias gariepinus) and zebra fish (Danio rerio). Environ. Toxicol. **16:**566–571.
36. **O'Brien, T. J., S. Ceryak, and S. R. Patierno.** 2003. Complexities of chromium carcinogenesis: role of cellular response, repair and recovery mechanisms. Mutat. Res. **533:**3–36.
37. **O'Hara, K. A., A. A. Nemec, J. Alam, L. R. Klei, B. T. Mossman, and A. Barchowsky.** 2006. Chromium (VI) inhibits heme oxygenase-1 expression in vivo and in arsenic-exposed human airway epithelial cells. J. Cell. Physiol. **209:**113–121.
38. **Ohm, J. E., K. M. McGarvey, X. Yu, L. Cheng, K. E. Schuebel, L. Cope, H. P. Mohammad, W. Chen, V. C. Daniel, W. Yu, D. M. Berman, T. Jenuwein, K. Pruitt, S. J. Sharkis, D. N. Watkins, J. G. Herman, and S. B. Baylin.** 2007. A stem cell-like chromatin pattern may predispose tumor suppressor genes to DNA hypermethylation and heritable silencing. Nat. Genet. **39:**237–242.
39. **Reynolds, M., E. Peterson, G. Quievryn, and A. Zhitkovich.** 2004. Human nucleotide excision repair efficiently removes chromium-DNA phosphate adducts and protects cells against chromate toxicity. J. Biol. Chem. **279:** 30419–30424.
40. **Salnikow, K., A. Zhitkovich, and M. Costa.** 1992. Analysis of the binding sites of chromium to DNA and protein in vitro and in intact cells. Carcinogenesis **13:**2341–2346.
41. **Santi, D. V., A. Norment, and C. E. Garrett.** 1984. Covalent bond formation between a DNA-cytosine methyltransferase and DNA containing 5-azacytosine. Proc. Natl. Acad. Sci. USA **81:**6993–6997.
42. **Santos-Rosa, H., and C. Caldas.** 2005. Chromatin modifier enzymes, the histone code and cancer. Eur. J. Cancer **41:**2381–2402.
43. **Shimada, T., and Y. Fujii-Kuriyama.** 2004. Metabolic activation of polycyclic aromatic hydrocarbons to carcinogens by cytochromes P450 1A1 and 1B1. Cancer Sci. **95:**1–6.
44. **Shumilla, J. A., R. J. Broderick, Y. Wang, and A. Barchowsky.** 1999. Chromium(VI) inhibits the transcriptional activity of nuclear factor-kappaB by decreasing the interaction of p65 with cAMP-responsive element-binding protein-binding protein. J. Biol. Chem. **274:**36207–36212.
45. **Talaska, G., K. L. Dooley, and F. F. Kadlubar.** 1990. Detection and characterization of carcinogen-DNA adducts in exfoliated urothelial cells from 4-aminobiphenyl-treated dogs by 32P-postlabelling and subsequent thin-layer and high-pressure liquid chromatography. Carcinogenesis **11:**639–646.
46. **Tian, Y., S. Ke, M. Chen, and T. Sheng.** 2003. Interactions between the aryl hydrocarbon receptor and P-TEFb. Sequential recruitment of transcription factors and differential phosphorylation of C-terminal domain of RNA polymerase II at cyp1a1 promoter. J. Biol. Chem. **278:**44041–44048.
47. **Uno, S., T. P. Dalton, S. Derkenne, C. P. Curran, M. L. Miller, H. G. Shertzer, and D. W. Nebert.** 2004. Oral exposure to benzo[a]pyrene in the mouse: detoxication by inducible cytochrome P450 is more important than metabolic activation. Mol. Pharmacol. **65:**1225–1237.
48. **Uno, S., T. P. Dalton, N. Dragin, C. P. Curran, S. Derkenne, M. L. Miller, H. G. Shertzer, F. J. Gonzalez, and D. W. Nebert.** 2006. Oral benzo[a]pyrene in Cyp1 knockout mouse lines: CYP1A1 important in detoxication, CYP1B1 metabolism required for immune damage independent of total-body burden and clearance rate. Mol. Pharmacol. **69:**1103–1114.
49. **Uno, S., T. P. Dalton, H. G. Shertzer, M. B. Genter, D. Warshawsky, G. Talaska, and D. W. Nebert.** 2001. Benzo[a]pyrene-induced toxicity: paradoxical protection in Cyp1a1(−/−) knockout mice having increased hepatic BaP-DNA adduct levels. Biochem. Biophys. Res. Commun. **289:**1049–1056.
50. **Wei, Y. D., K. Tepperman, M. Y. Huang, M. A. Sartor, and A. Puga.** 2004. Chromium inhibits transcription from polycyclic aromatic hydrocarbon-inducible promoters by blocking the release of histone deacetylase and preventing the binding of p300 to chromatin. J. Biol. Chem. **279:**4110–4119.
51. **Wells, J., and P. J. Farnham.** 2002. Characterizing transcription factor binding sites using formaldehyde crosslinking and immunoprecipitation. Methods **26:**48–56.
52. **Wetterhahn, K. E., and J. W. Hamilton.** 1989. Molecular basis of hexavalent chromium carcinogenicity: effect on gene expression. Sci. Total Environ. **86:**113–129.
53. **Whitlock, J. P., Jr.** 1999. Induction of cytochrome P4501A1. Annu. Rev. Pharmacol. Toxicol. **39:**103–125.
54. **Xu, J., F. C. Manning, and S. R. Patierno.** 1994. Preferential formation and repair of chromium-induced DNA adducts and DNA-protein crosslinks in nuclear matrix DNA. Carcinogenesis **15:**1443–1450.
55. **Zhang, Y., N. Fatima, and M. L. Dufau.** 2005. Coordinated changes in DNA methylation and histone modifications regulate silencing/derepression of luteinizing hormone receptor gene transcription. Mol. Cell. Biol. **25:**7929–7939.
56. **Zhitkovich, A.** 2005. Importance of chromium-DNA adducts in mutagenicity and toxicity of chromium(VI). Chem. Res. Toxicol. **18:**3–11.
57. **Zhitkovich, A., and M. Costa.** 1992. A simple, sensitive assay to detect DNA-protein crosslinks in intact cells and in vivo. Carcinogenesis **13:**1485–1489.